

Oscillating field current drive experiments in a reversed field pinch

K. F. Schoenberg, J. C. Ingraham, C. P. Munson, P. G. Weber, D. A. Baker, R. F. Gribble, R. B. Howell, G. Miller, W. A. Reass, A. E. Schofield, S. Shinohara,^{a)} and G. A. Wurden

Los Alamos National Laboratory, Los Alamos, New Mexico 87545

(Received 20 January 1988; accepted 4 May 1988)

Steady-state current sustainment by oscillating field current drive (OFCD) utilizes a technique in which the toroidal and poloidal magnetic fields at the plasma surface are modulated at audio frequencies in quadrature. Experiments on the ZT-40M reversed field pinch [Fusion Technol. 8, 1571 (1985)] have examined OFCD over a range of modulation amplitude, frequency, and phase. For all cases examined, the magnitude of the plasma current is dependent on the phase of the modulations as predicted by theory. However, evidence of current drive has only been observed at relatively low levels of injected power. For larger modulation amplitudes, the data suggest that substantial current drive is offset by increased plasma resistance as a result of modulation enhanced plasma-wall interactions. The initial experimental results and supporting theoretical interpretations of OFCD are discussed.

I. INTRODUCTION

Oscillating field current drive (OFCD) is a current drive technique in which the toroidal and poloidal magnetic fields at the plasma surface are modulated at audio frequencies in quadrature.¹⁻³ In the reversed field pinch (RFP), the plasma's nonlinear response to these modulations is predicted to maintain the mean magnetoplasma configuration, and hence the plasma current. Because OFCD holds promise for relatively simple, noninvasive, and efficient current drive in high temperature, high density plasmas, it has been adopted as the primary current drive technique in two major RFP reactor studies.^{4,5} In addition, OFCD may be applicable to other toroidal confinement systems, provided appropriate "relaxation" mechanisms exist.^{6,7}

The OFCD concept was initially studied by simulating the effect of ac magnetic field modulations on the ZT-40M⁸ RFP experiment.² In these zero-dimensional (0-D) simulations, which utilize radial integrals over the mean axisymmetric field profiles, the plasma was assumed to evolve through a series of quasirelaxed states determined by the modified force-free equation $\nabla \times \mathbf{B} = \lambda \mathbf{B}$, where λ is a function of the minor radius and specifies the parallel current density profile ($\lambda = \mu_0 \mathbf{J} \cdot \mathbf{B} / B^2$). (This force-free formalism provides a good approximation to RFP mean field behavior even with finite beta.⁹) The simulations predicted that OFCD could be demonstrated on ZT-40M provided the plasma relaxation time was shorter than one modulation period, and the field modulation process did not significantly increase discharge resistivity.

These provisos were experimentally investigated on ZT-40M by measuring plasma response to single field modulations.¹⁰ The plasma relaxation time was measured at $\approx 100 \mu\text{sec}$, which is substantially shorter than a required field modulation period for OFCD demonstration. In addition, the measurements also showed that during the single field modulation, no obvious deleterious effects were apparent provided the toroidal field reversal was adequately maintained.

^{a)} University of Tokyo, Tokyo, Japan.

Based on these positive indicators, a phase controlled, multimewatt dual oscillator was constructed to demonstrate and study current drive during 50–180 kA discharges, and to assess the potential of OFCD for future devices. In this paper we present the initial results from this experimental study.

II. THE OFCD POWER SYSTEM

Figure 1 illustrates a schematic of the ZT-40M OFCD apparatus.¹¹ At the heart of the system are two 20 MVA oscillators, which are directly coupled to the toroidal and poloidal magnetic field circuits. Each oscillator consists of a tank circuit driven by 20 parallel ML8618 power triodes in class D operation. Proper power and phasing of the oscillators are set by a phase controller, which adjusts both the grid drive waveform timing, and conduction angle of the power triodes. The system base operating frequency is set by tuning the tank circuit inductance and/or capacitance, and is adjustable from 1 to 5 kHz.

III. EXPERIMENTAL STUDIES

A. Introduction

For a given RFP discharge, current drive by OFCD is directly controlled by five parameters: the amplitude of the ac modulating voltages referenced to the plasma surface, v_θ and v_ϕ , the phase lag δ of v_ϕ with respect to v_θ , the driving frequency ν , and the pinch operating point Θ_0 [Θ is defined as the poloidal magnetic field at the plasma edge $B_\theta(a)$ divided by the mean toroidal field $\langle B_\phi \rangle$]. Optimizing OFCD performance with respect to these parameters is driven by both physics considerations and machine operational characteristics, as described below.

From a physics standpoint based on the 0-D simulations, the driving modulation period ν^{-1} must be longer than the plasma relaxation time and shorter than the resistive plasma current decay time. In ZT-40M, this constrains ν to lie between 500 Hz and 5 kHz. In addition, from an operational standpoint, electromagnetic shielding by the ZT-40M metallic vacuum vessel also limits the upper modula-

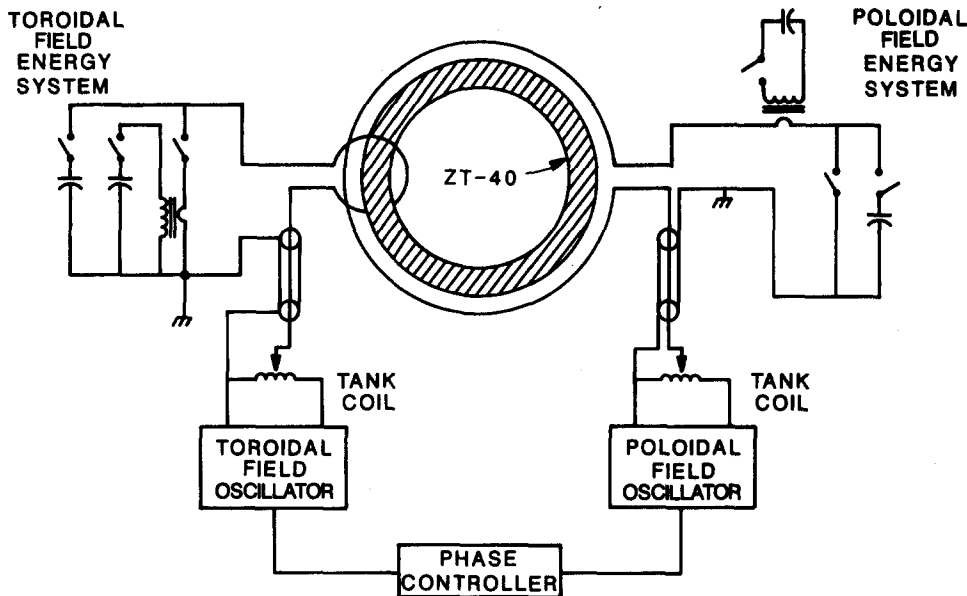


FIG. 1. ZT-40M OFCD schematic.

tion frequency to under 5 kHz, and the temporal characteristics of magnetic sawtooth oscillations¹² sets a lower frequency limit of approximately 2 kHz. These considerations constrain the ZT-40M OFCD discharges in the range $2 \text{ kHz} < \nu < 5 \text{ kHz}$.

The choice of the operating point Θ_0 is driven by two conflicting considerations. First, optimal OFCD performance requires a minimal plasma resistance. For fixed discharge conditions in ZT-40M, this occurs for rather shallow toroidal field reversal and low Θ operation ($\Theta_0 \approx 1.45$). Second, in order to maximize drive power into the toroidal field modulation, the ν_θ modulation should be maximized. This consideration requires RFP operation at high Θ in order to maintain reversal. However, high Θ operation on ZT-40M results in substantial magnetic sawtooth activity and an increase in the plasma resistance. In light of these conflicting considerations, Θ was constrained in the range $\Theta_0 = 1.5 \pm 0.2$ over most of the OFCD discharges studied.

In principle, there is considerable flexibility in balancing the relative amplitudes of ν_θ and ν_ϕ , provided sufficient total power is supplied by the modulations to drive current against resistive losses. In practice, however, the operating constraint on Θ_0 and maintenance of toroidal field reversal directly limits the allowed poloidal voltage modulation. As a result, the ν_θ channel generally supplies only $\approx 20\%$ of the total ac power injected. Finally, both the 0-D simulations² and simple models based on global magnetic helicity balance¹ predict optimal current drive when ν_ϕ lags ν_θ by $\pi/2$ rad at the plasma surface ($\delta = \pi/2$).

B. High power modulation experiments

To date, the OFCD experimental results on ZT-40M may be dichotomized into two categories. High power modulations of 180–200 kA discharges, and low power modulations of 50–70 kA discharges. Figure 2 is illustrative of the high power injection results. The nonmodulated curve displays a nominally flattopped 180 kA discharge, which is maintained by a dc input power of approximately 7 MW. The modulated traces display the results of applying sinusoi-

dal voltages to the toroidal and poloidal field circuits, but with different relative phases. For the dotted modulation curves, labeled “drive,” ν_ϕ lags ν_θ by $\pi/2$ ($\delta = \pi/2$). The solid modulation curves, labeled “antidrive,” were obtained setting $\delta = -\pi/2$. In both cases, the input drive power during modulation peaks at roughly 80 MVA, with an rms input to the discharge of approximately 20 MW.

In all OFCD discharges examined, there is a strong and demonstrable dependence of plasma response on δ which is in agreement with the 0-D simulations and analytic theory based on global magnetic helicity balance.^{1–3} However, in analyzing the behavior of high power OFCD discharges, one concludes that the failure to increase the plasma current when $\delta = \pi/2$ results directly from modulation enhanced plasma-wall interactions (PWI). Specifically, for the cases shown, the energy deposited on a bolometer between 6 and 10 msec is 15 kJ for the baseline case, 17 kJ for the drive case, and 22 kJ for the antidrive case. The incremental radiated energy for the antidrive case is comparable to the incremental energy applied to the plasma by the oscillating fields. The

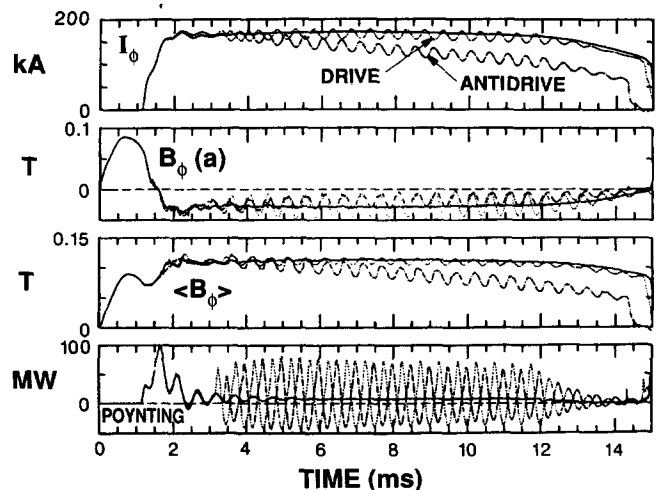


FIG. 2. High power OFCD discharges at 2 kHz.

average metal line emission (CrI at the wall) tracks the radiated power as a function of δ , which implies that the enhanced plasma-wall interactions are responsible for the larger radiated power losses observed during the modulated discharges.

A further PWI observation is that the CrI emission is strongly correlated with the magnitude of the reversed field at the wall when one either increases or decreases F from its optimum value [$F_o \equiv B_\phi(a)/\langle B_\phi \rangle = -0.15$ and $\Theta_o = 1.4$]. For example, for standard unmodulated discharges, where F is between -0.1 and -0.2 , the CrI influx is constant. However, at $F = -0.3$, the CrI influx increases by roughly 50%. Figure 3 compares the temporal history of CrI emission with the input Poynting power and toroidal field at the wall for the three OFCD cases. As one drives high power OFCD discharges, the toroidal field reversal at the wall is modulated over a rather large range. The resulting time averaged CrI influx is typically 30% higher for drive and

100% higher for antidrive when compared with the unmodulated baseline discharges. In addition, note the strong correlation between increases in CrI emission and the minimum absolute values of $B_\phi(a)$.

The observed increase in plasma impurity content (and concomitant increase in plasma resistance) during modulation adversely affects the current drive process. For example, for the drive discharge illustrated in Fig. 2, 0-D simulations calculate that a 10%–15% increase in the global plasma resistance is necessary to match the experimental results. In other words, a 10%–15% increase in global plasma resistance is sufficient to negate an observable current drive effect at the applied levels of OFCD power (modulations).

Spectroscopy has also been used to examine whether the plasma response to the driven modulations is toroidally symmetric. During modulation, it is observed that there are characteristic emission pulses of CrI and D_α radiation that are synchronous with the modulated power. However, the relative amplitudes of these emissions at various toroidal locations are not reproducible. (This nonaxisymmetry has also been observed during standard unmodulated discharges at high Θ .¹³) Hence the plasma-wall interactions are probably not toroidally symmetric, which can result in a nonaxisymmetric plasma response to OFCD. The global effect of this asymmetry on OFCD performance is presently uncertain.

To access the widest possible operational regime, OFCD discharges were also modulated at 5 kHz. This is the maximum modulation frequency that can penetrate the metal vacuum vessel without excessive power loss. The results of the 5 kHz operation were similar to those at lower frequencies in that there was a strong dependence of plasma response on phase, and the current drive effect was countered by increased plasma-wall interactions.

C. Low power modulation experiments

In order to mitigate the enhanced plasma-wall interactions observed during high power modulation discharges, low power modulations (≈ 7 MVA) of 60–70 kA “ramped” discharges¹⁴ were examined. For these low current discharges, less current drive effect was expected because of the lower injected ac power and higher baseline resistivity. However, it was anticipated that the lower wall loading inherent in low current operation, as well as the increased inward Poynting vector and its associated inwardly directed plasma drifts during the ramp, would reduce the PWI effects relative to the OFCD.

Figure 4 is illustrative of the lower power injection results. The three traces denote baseline (unmodulated), drive (modulated dotted), and antidrive (modulated solid) discharges. For these discharges, based on spectroscopy and global resistivity calculations, there is no significant increase in plasma resistivity between the baseline and current drive discharges. As shown in Fig. 5, the integrated D_α emission, which is an indication of plasma-wall interactions, the total integrated radiated power, and the line averaged plasma density are roughly equivalent for the three discharge cases.

Again, the plasma current response to the voltage mod-

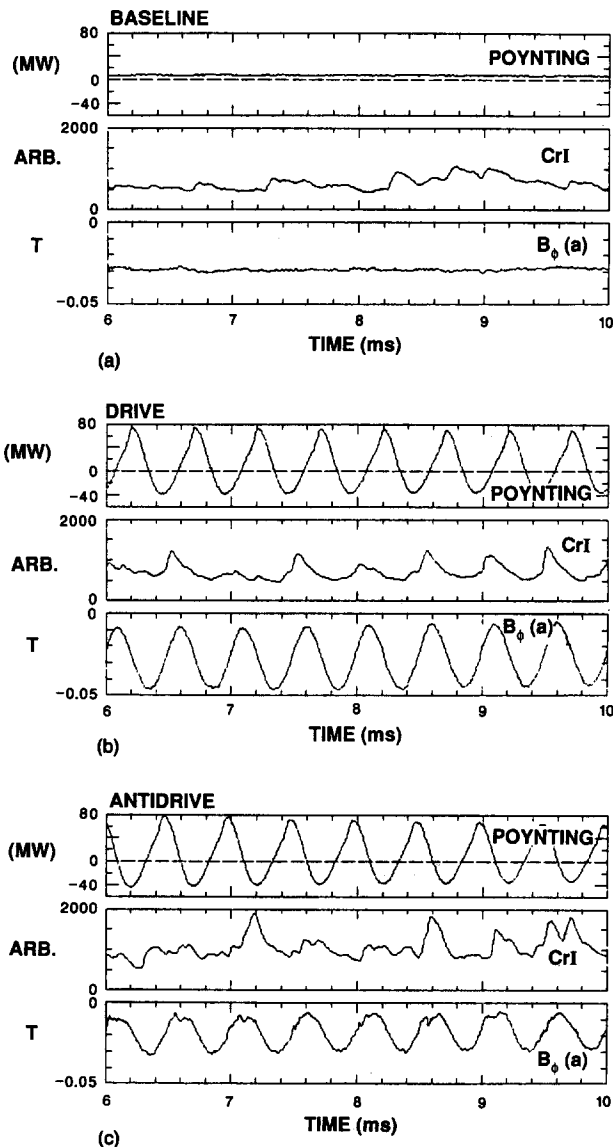


FIG. 3. Input Poynting power, CrI emission, and toroidal field at the wall $B_\phi(a)$ for three high power OFCD discharges: (a) baseline, (b) drive, and (c) antidrive.

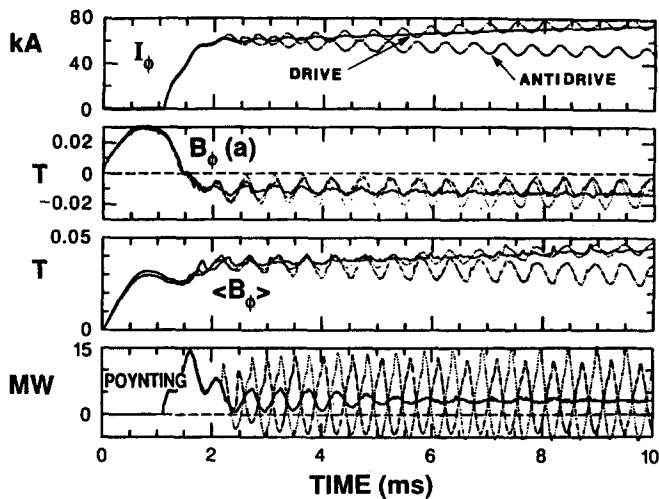


FIG. 4. Low power OFCD discharge at 2 kHz.

ulation phasing is in agreement with magnetic helicity and 0-D simulation predictions. In addition, a small current drive effect (approximately 5%), manifested by a small increase in plasma current (Fig. 4) and small decrease in input volt-seconds (Fig. 6), is observed during OFCD discharges with optimal drive phasing. Under the assumption that the baseline resistivity is unchanged, this 5% effect agrees with the current drive predictions of the 0-D model to within the experimental measurement uncertainties.

As the modulated power was increased above the values of Fig. 4, the chromium influx from the wall also increased. The particle confinement time was observed to decrease slowly as a function of increasing modulation amplitude. The soft x-ray flux also dropped as a function of modulation amplitude, indicating a possible reduction in electron temperature. Concomitantly, the volume averaged plasma resistivity, based on global magnetic helicity balance,⁹ was observed to increase.

In summary, the best OFCD performance from a spectroscopic and resistivity viewpoint occurs when the drive phase angle $\delta = \pi/2$, and at modulation amplitudes equal to or below the values shown in Fig. 4. At these low levels of modulation, there is no significant increase in the global plasma resistance between the baseline and current drive discharges. Deviation from these conditions results in plasma degradation. However, at these low levels of modulation, the expected current drive effect is limited to roughly 5%.

D. Mean magnetic field behavior

One further observation, which directly supports an assumption implicit in the 0-D simulation predictions of OFCD, relates to the temporal and spatial behavior of the mean magnetic fields during modulation. In the 0-D simulations, the plasma is assumed to evolve through a series of quasirelaxed states, described by the modified Bessel function model (MBFM).^{15,16} For the low current discharges, the mean fields were measured using an internal magnetic probe that simultaneously measured B_θ and B_ϕ at ten equally spaced radial positions spanning the plasma's radial extent.¹⁷

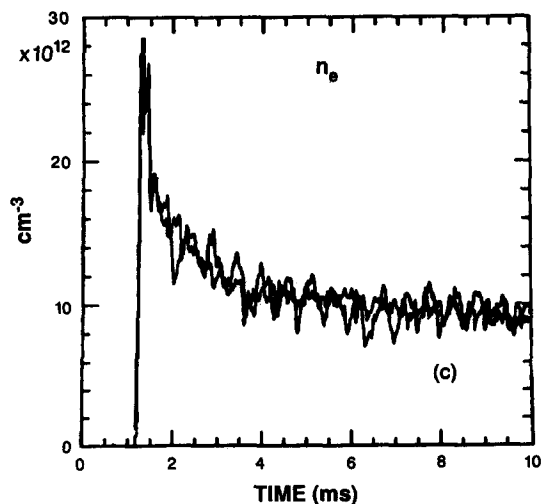
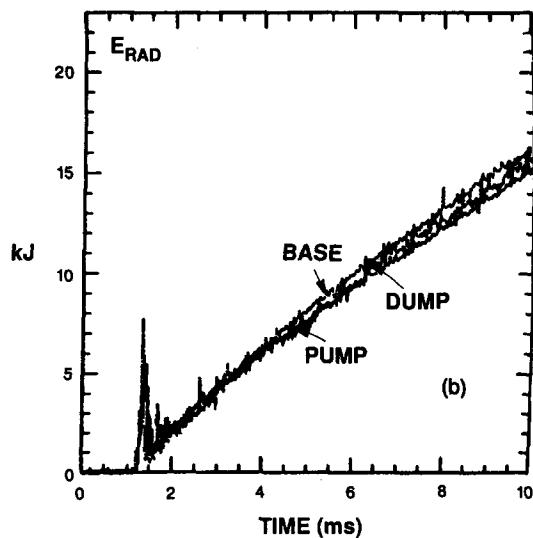
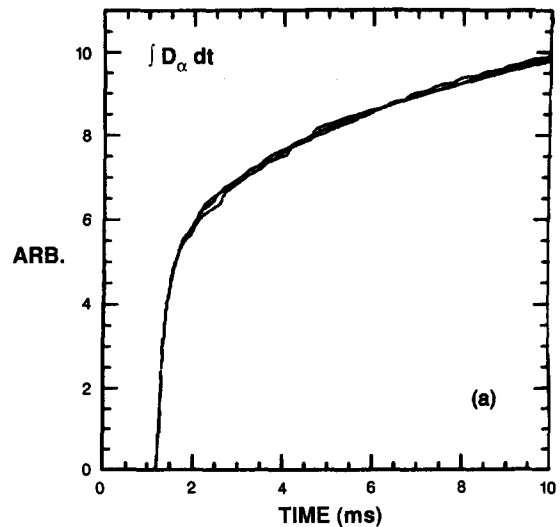


FIG. 5. Time integrated radiated power and density for three low power OFCD discharges: (a) time integrated D_α emission, (b) total energy radiated, and (c) an overlay of line averaged plasma density comparing drive and baseline discharges. In this figure, the curves labeled pump and dump correspond to drive and antidrive discharges, respectively.

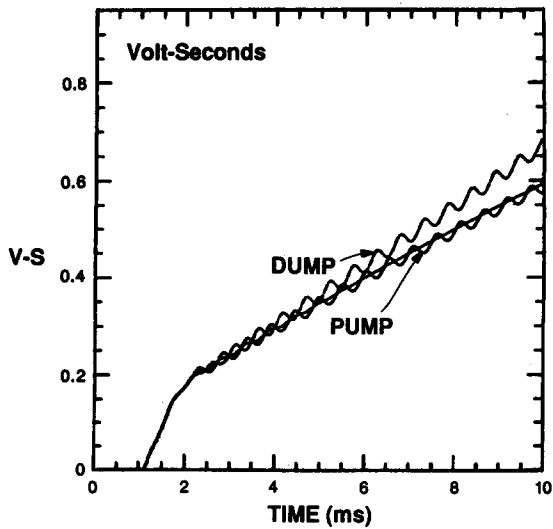


FIG. 6. Input volt-seconds for the low power OFCD discharges of Fig. 4. The unmodulated curve denotes the baseline; pump and dump refer to drive and antidrive, respectively.

The measured profiles as a function of time are shown in Fig. 7 for the current drive case ($\delta = \pi/2$). For this case, the measurements were made for a discharge current of 50 kA, an OFCD modulation frequency of 2 kHz, and a discharge pulse length of 5 msec (to minimize probe heating). The 15% modulation of B_ϕ on axis is in phase with the plasma current, and π rad out of phase relative to B_ϕ at the edge.

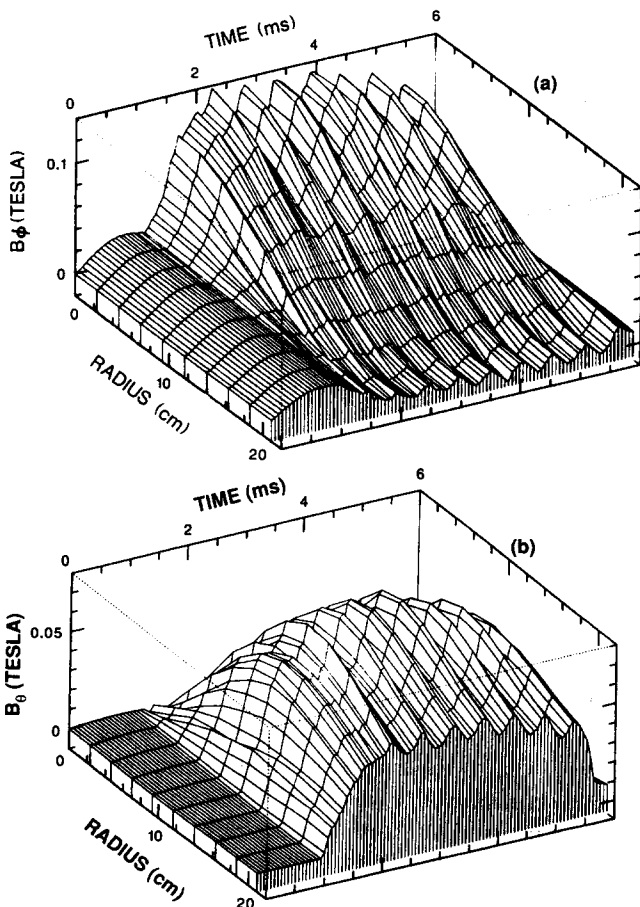


FIG. 7. Temporal behavior of the profiles of (a) $B_\phi(r)$ and (b) $B_\theta(r)$ during an OFCD current drive discharge.

The amplitude of the B_ϕ modulation on axis, as well as its phase relationship with the driven field at the edge, are in good quantitative agreement with what one would expect if the mean magnetic fields remain in the "quasirelaxed" (MBFM) state during modulation. Similar quantitative agreement between the data and the MBFM predictions is found for the current density on axis, and for the ratio of the current density to the field on axis $\lambda(0)$. This agreement between the measurements and the simulation predictions over the whole field profile is demonstrated in Fig. 8, where the measurements and MBFM predictions are compared at the times of maximum and minimum toroidal plasma current in the modulation cycle. The predicted field profiles were calculated using the MBFM model with a constant normalized cutoff radius of 0.6,¹⁶ and with field values adjusted to fit the externally measured toroidal flux and the pinch parameter (\odot). For this case, $\langle \lambda(0) \rangle = 17.0 m^{-1} \pm 4\%$, $\langle \odot \rangle = 1.71 \pm 11\%$ in phase with I_ϕ , and $\langle F \rangle = -0.34 \pm 70\%$ out of phase with I_ϕ (i.e., F goes more negative as I_ϕ goes more positive).

IV. THEORETICAL INTERPRETATIONS

The experimental current drive studies, discussed above, were initially motivated by magnetic helicity arguments.^{1,18} The concept of magnetic helicity, however, is not necessary for explaining current drive in the RFP. Any process that results in partial relaxation of the mean fields has the potential for driving current without consuming the time-averaged poloidal flux. Although the physical mechanisms responsible for this partial relaxation have not been

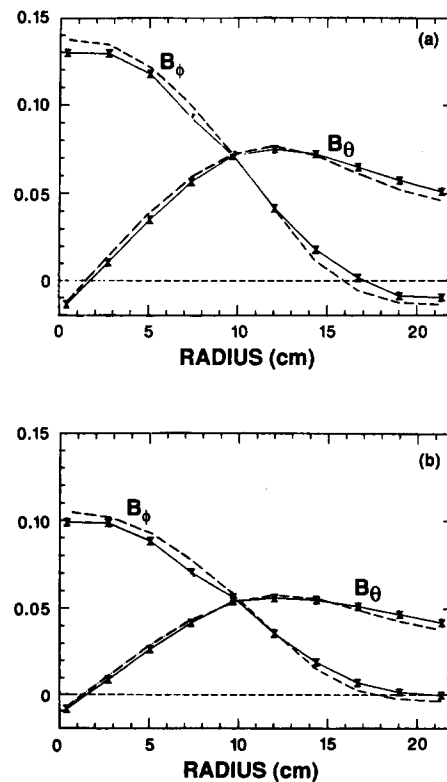


FIG. 8. Comparison of field profile measurements (\times) and MBFM predictions (---) for maximum (a) and minimum (b) compression during OFCD.

unambiguously identified, possible candidates include resistive magnetohydrodynamics (MHD), stochastic fields¹⁹ with kinetic effects,²⁰ resistive evolution with closed or imperfect flux surfaces,^{21,22} helical Ohmic states,^{23,24} nonaxisymmetric field errors,²⁵ the nonlinear Hall effect,²⁶ stepped relaxation,²⁷ or plasma turbulence.

Despite the uncertainty in RFP relaxation physics, it has been possible to simulate accurately the OFCD experimental results with the 0-D model.² In this model, relaxation physics is embodied in the constraint that the RFP operate along a well defined trajectory in $F\text{-}\odot$ phase space. The exact shape of this trajectory is dependent on how “relaxed” the fields are during modulation. For example, if the modulation period is long compared to the plasma relaxation time (τ_R), the mean fields are considered “relaxed” and the dynamic $F\text{-}\odot$ trajectory during modulation is approximately linear. On the other hand, if the modulation period is comparable to τ_R , the mean fields are “partially relaxed,” and the trajectory is elliptical.²⁸ Although the 0-D model has simulated current drive for both complete and partial relaxation conditions,²⁸ the modulation period in these simulations always exceeded τ_R . Both types of relaxation behavior have been observed during the course of the OFCD experiments.

Although the 0-D model is a valuable design and analysis tool, it cannot self-consistently ascertain the role of internal plasma dynamics on the OFCD process. To address this issue, the most fully developed and extensively studied models utilize resistive MHD computer codes. However, noting that fully 3-D calculations are both expensive and time consuming, recent advances in MHD parameter studies of OFCD have been made possible by the development of a correction term to Ohm’s law from quasilinear MHD resistive tearing mode theory.^{29,30} This correction term, called hyper-resistivity, has been incorporated into 1-D cylindrical and 2-D toroidal MHD codes, and involves a diffusion coefficient \mathcal{D} that depends on the radial amplitudes of the fluctuating Fourier MHD modes, and a second spatial derivative of the mean field value of λ . The effect of this diffusive term is to flatten the λ profile at a rate that depends on \mathcal{D} . It has been shown that under certain assumptions, this term dissipates energy while conserving magnetic helicity.^{31,32,30}

Parameter studies^{33–35} of OFCD with a 1-D hyper-resistivity code have been made where the \mathcal{D} profile was determined by computing the fluctuation amplitudes without oscillating fields from a fully nonlinear 3-D pseudospectral resistive MHD code.³⁶ These simulations showed a similar response to that obtained experimentally. In particular, a large hysteresis was seen in the $F\text{-}\odot$ trajectories for 120 kA discharges. (Small hysteresis was also observed for 50 kA discharges.) Several expensive simulations of OFCD were also run using the full 3-D code directly, and qualitative agreement with the 1-D hyper-resistivity simulations was obtained.

The 1-D hyper-resistive and 3-D nonlinear MHD studies have also provided qualitative recommendations for further experimental study. With these simulations, it has been possible to obtain current drive for ZT-40M plasma parameters when the driving frequency is comparable to or shorter than the inverse hyper-resistive relaxation time. It

should be noted that this is in contrast to the predictions of the 0-D model, where the plasma remains quasirelaxed during modulation. For ZT-40M, a proper “hyper-resistive drive” requires ν to exceed 10 kHz. This frequency range is presently experimentally untenable as a result of the shielding effect of the metallic vacuum vessel. Nevertheless, the hyper-resistive study emphasizes the potential importance of the driving frequency in obtaining successful OFCD operation if hyper-resistivity effects correctly model the underlying physics.

Further investigation into the physical mechanisms associated with OFCD have been made using standard 1-D transport and linear stability studies.³⁷ These studies have shown that $m = 1$ modes are required for current drive within the context of the resistive MHD model, and have identified a class of $m = 1$ modes that can generate the required poloidal flux for current drive. These current drive modes are driven unstable by plasma compression during the first half-cycle of modulation that drives an off axis current peak in λ . The compression driven perturbation is then reconfigured by a Kadomtsev-like reconnection³⁸ that flattens λ with a resulting increase in poloidal flux.

V. CONCLUSIONS

In conclusion, OFCD experiments on ZT-40M have met with mixed success. On one hand, there is a strong and demonstrable dependence of plasma response on the modulation phasing δ that is in agreement with magnetic helicity models and 0-D simulation predictions. This agreement is further strengthened by the measured spatial and temporal behavior of the mean magnetic fields during modulation.

On the other hand, a clear demonstration of substantial current drive in a low temperature (≈ 200 eV) plasma by OFCD is problematic. In ZT-40M, which operates with a bare metallic wall and minimal wall protection, plasma-wall interactions dominate the discharge physics at the level of current and modulation amplitude necessary to provide a definitive current drive demonstration. For that reason, as well as constraints imposed by present operational considerations, only a small current drive effect has been observed during low current, low modulation discharges. Although the investigation of techniques to increase current drive by OFCD on ZT-40M will continue, an unambiguous demonstration of OFCD may require the substantially improved wall protection and plasma resistivity characteristics anticipated in the next generation of RFP experiments.

ACKNOWLEDGMENTS

The authors wish to acknowledge the entire Los Alamos RFP team for its contributions to the construction, operation, and measurements that were necessary for the OFCD experiments. In addition, we wish to explicitly acknowledge Mr. C. Hammer for electrical engineering and construction support, Dr. J. Phillips for discussions and cross-checking of data, and Dr. R. Moses, Dr. R. Nebel, and Dr. M. Bevir for their suggestions and discussion.

- ¹See National Technical Information Service Document No. DE82008957 (Los Alamos National Laboratory Report LA-8944-C, 1981, by M. K. Bevir and J. W. Gray). Copies may be ordered from the National Technical Information Service, Springfield, Virginia 22161. The price is \$32.95 plus a \$3.00 handling fee. All orders must be prepaid.
- ²K. F. Schoenberg, R. F. Gribble, and D. A. Baker, *J. Appl. Phys.* **56**, 2519 (1984).
- ³M. K. Bevir, C. G. Gimblett, and G. Miller, *Phys. Fluids* **28**, 1826 (1985).
- ⁴See National Technical Information Service Document No. DE85002351 (Los Alamos National Laboratory Report LA-10200-MS, 1984, by R. L. Hagenson, R. A. Krakowski, C. G. Bathke, R. L. Miller, M. J. Embrechts, N. M. Schnurr, M. E. Battat, R. J. LaBauve, and J. W. Davidson). Copies may be ordered from the National Technical Information Service, Springfield, Virginia 22161. The price is \$38.95 plus a \$3.00 handling fee. All orders must be prepaid.
- ⁵See National Technical Information Service Document No. DE87010508 (UCLA Report UCLA-PPG-1100, 1987, by F. Najmabadi, N. M. Ghoniem, R. W. Conn, and the Titan Design Team). Copies may be ordered from the National Technical Information Service, Springfield, Virginia 22161. The price is \$38.95 plus a \$3.00 handling fee. All orders must be prepaid.
- ⁶J. T. Hogan, *Bull. Am. Phys. Soc.* **31**, 1548 (1986).
- ⁷P. M. Bellan, *Bull. Am. Phys. Soc.* **32**, 1747 (1987).
- ⁸R. S. Massey, R. G. Watt, P. G. Weber, G. A. Wurden, D. A. Baker, C. J. Buchenauer, T. Cayton, J. N. DiMarco, J. N. Downing, R. M. Erickson, R. F. Gribble, A. Haberstick, R. B. Howell, J. C. Ingraham, E. M. Little, G. Miller, C. P. Munson, J. A. Phillips, M. M. Pickrell, K. F. Schoenberg, A. E. Schofield, and D. M. Weldon, *Fusion Technol.* **8**, 1571 (1985).
- ⁹K. F. Schoenberg, R. W. Moses, Jr., and R. L. Hagenson, *Phys. Fluids* **27**, 1671 (1984).
- ¹⁰K. F. Schoenberg, C. J. Buchenauer, R. S. Massey, J. G. Melton, R. W. Moses, R. A. Nebel, and J. A. Phillips, *Phys. Fluids* **27**, 548 (1984).
- ¹¹W. A. Reass, R. F. Gribble, and C. F. Hammer, in *Proceedings of the 11th Symposium of Fusion Engineering* (IEEE, New York, 1985), Vol. II, p. 1214.
- ¹²R. G. Watt and R. A. Nebel, *Phys. Fluids* **26**, 1168 (1983).
- ¹³R. B. Howell, J. C. Ingraham, G. A. Wurden, P. G. Weber, and C. J. Buchenauer, *Phys. Fluids* **30**, 1828 (1987).
- ¹⁴See National Technical Information Service Document No. DE84015076 (Los Alamos National Laboratory Report LA-10060-MS, 1984, by J. A. Phillips, D. A. Baker, L. C. Burkhardt, R. M. Erickson, A. Haberstick, J. C. Ingraham, E. M. Little, J. G. Melton, K. F. Schoenberg, R. G. Watt, P. G. Weber, and G. A. Wurden). Copies may be ordered from the National Technical Information Service, Springfield, Virginia 22161. The price is \$9.95 plus a \$3.00 handling fee. All orders must be prepaid.
- ¹⁵J. W. Johnston, *Plasma Phys.* **23**, 127 (1981).
- ¹⁶K. F. Schoenberg, R. F. Gribble, and J. A. Phillips, *Nucl. Fusion* **22**, 1433 (1982).
- ¹⁷See National Technical Information Service Document No. DE84003704 (Los Alamos National Laboratory Report LA-9613-MS, 1983, by L. C. Burkhardt). Copies may be ordered from the National Technical Information Service, Springfield, Virginia 22161. The price is \$9.95 plus a \$3.00 handling fee. All orders must be prepaid.
- ¹⁸T. Jensen and M. S. Chu, *Phys. Fluids* **27**, 2881 (1984).
- ¹⁹M. G. Rusbridge, *Plasma Phys.* **19**, 499 (1977).
- ²⁰A. R. Jacobson and R. W. Moses, *Phys. Rev. A* **29**, 3335 (1984).
- ²¹G. Miller, *Phys. Fluids* **28**, 1354 (1985).
- ²²G. Miller, *Phys. Fluids* **31**, 1133 (1988).
- ²³A. Sykes and J. A. Wesson, in *Proceedings of the 8th European Conference on Controlled Fusion and Plasma Physics* (European Physical Society, Budapest, 1977), Vol. 1, p. 80.
- ²⁴See National Technical Information Service Document No. DE82008957 (Los Alamos National Laboratory Report LA-8944-C, 1981, by C. G. Gimblett). Copies may be ordered from the National Technical Information Service, Springfield, Virginia 22161. The price is \$32.95 plus a \$3.00 handling fee. All orders must be prepaid.
- ²⁵A. R. Jacobson, *Phys. Fluids* **27**, 7 (1984).
- ²⁶M. L. Xne and D. Brotherton-Ratcliffe, *Plasma Phys. Controlled Fusion* **29**, 287 (1987).
- ²⁷J. M. Finn, *Phys. Fluids* **29**, 2630 (1986).
- ²⁸See National Technical Information Service Document No. DE84015090 (Los Alamos National Laboratory Report LA-9161-MS, 1984, by K. F. Schoenberg, R. F. Gribble, and D. A. Baker). Copies may be ordered from the National Technical Information Service, Springfield, Virginia 22161. The price is \$12.95 plus a \$3.00 handling fee. All orders must be prepaid.
- ²⁹H. R. Strauss, *Phys. Fluids* **28**, 2786 (1985).
- ³⁰E. Hameiri and A. Bhattacharjee, *Phys. Fluids* **30**, 1743 (1987).
- ³¹M. J. Schaffer, *Bull. Am. Phys. Soc.* **30**, 1405 (1985).
- ³²A. H. Boozer, *J. Plasma Physics* **35**, 133 (1986).
- ³³D. S. Harned, D. D. Schnack, H. R. Strauss, and R. A. Nebel, submitted to *Phys. Fluids*.
- ³⁴H. R. Strauss and D. S. Harned, *Phys. Fluids* **30**, 164 (1987).
- ³⁵R. A. Nebel, K. A. Werley, R. A. Scardovelli, G. H. Miley, D. S. Harned, H. R. Strauss, D. D. Schnack, and Z. Mikic, in *Plasma Physics and Controlled Nuclear Fusion Research, 1986* (IAEA, Vienna, 1987), Vol. II, p. 701.
- ³⁶D. D. Schnack, D. C. Barnes, S. Mikic, D. S. Harned, and E. J. Caramana, *J. Comput. Phys.* **70**, 330 (1987).
- ³⁷R. Scardovelli, R. Nebel, K. A. Werley, and G. H. Miley, submitted to *Phys. Fluids*.
- ³⁸B. Kadomtsev, *Sov. J. Plasma Phys.* **1**, 389 (1975).
- ³⁹E. J. Caramana, R. A. Nebel, and D. D. Schnack, *Phys. Fluids* **25**, 1305 (1983).